Available online at www.rajournals.in

RA JOURNAL OF APPLIED RESEARCH
ISSN: 2394-6709
DOI:10.47191/rajar/v10i08.01
Volume: 10 Issue: 08 August-2024

International Open Access

Impact Factor- 8.174

Page no.- 161-177

Model for the Prediction of Performance Behavior of a Solid Oxide Electrolyte Fuel Cell

Sarwan S. Sandhu[1*], Kevin R. Hinkle[2]
[1,2]University of Dayton, Department of Chemical and Materials Engineering, 300 College Park, Dayton, OH 45469, USA

ARTICLE INFO

Published Online:
03 August 2024

ABSTRACT

The fundamental principles of thermodynamics, electrochemistry, transport phenomena, and chemical engineering science have been used to assemble and develop the formulation presented in this article. The formulation can be employed to predict the electrical performance behavior of a high temperature solid oxide electrolyte fuel cell (SOEFC) with respect to, for example, the cell Nernst electrical voltage, actual(terminal) cell voltage, total cell voltage loss, electric voltage efficiency; the maximum, actual and Carnot cycle engine thermal efficiencies; and the ratio of the reversible heat to the total cell reaction thermal energy production. Some of the conclusions drawn from the predicted data, with hydrogen as the fuel feed to a SOEFC, are as follows:

1) The Nernst open-cell electric potential decreases with an increase in the temperature from 800 to 1100 K.
2) The cell electric potential decreases with an increase in the hydrogen fractional conversion.
3) The cell open-circuit electric potential is higher at a higher cathode-side oxidant (air) total pressure.
4) The total cell voltage loss increases linearly with an increase in the geometric current density at
lower current densities; nonlinearly at higher current densities.
5) Ratio of the reversible thermal energy production (associated with the overall cell reaction entropy change) to the thermal energy production (associated with the overall cell reaction enthalpy change) increases almost linearly over the temperature range 800-1100 K.

Corresponding Author:
Sarwan S. Sandhu

KEYWORDS: SOFC, electrode kinetics, cell voltage loss, oxide anion transport, thermal energy production

1. INTRODUCTION

A solid oxide electrolyte fuel cell (SOFC) is composed of various components, all of which exist in the solid phase. Several characteristics of SOFCs which are attractive for utility and industrial applications [1,2] are listed below.

1. All fuel compositions; for example, pure hydrogen, carbon monoxide, natural gas or syn-gas (a mixture of equal mole fractions of carbon monoxide and hydrogen); can be oxidized spontaneously to thermodynamic completion if an adequate amount of air is supplied on the cathode side of a SOFC at a high cell operational temperature, e.g. $1000\ °C$).
2. Expensive electrocatalysts are not required because of the occurrence of the overall cell reaction at a high temperature. The direct processing of a fuel, for example,
$CH_4\ (g) + H_2O\ (g) \rightarrow CO\ (g) + 3H_2\ (g)$ is permitted. In the absence of major ohmic IR-voltage drops (i.e. the cell voltage losses associated with the transport of electrons and ions in the various cell components), they can be operated at much higher current densities than the molten carbonate fuel cells with high fuel conversion efficiency.
3. Operation of a SOFC is based on the oxide ion (O^{2-}) transport rather than transport of a fuel-derived ion. Therefore, a SOFC can be employed to oxidize any gaseous fuel.

4. Because of high temperature operation and tolerance to impure fuel streams, the SOFCs are attractive when coupled with coal gasification plants.
5. The solid oxide electrolyte (e.g. yttria (Y_2O_3 (s)) stabilized zirconia (ZrO_2 (s))) is very stable. Therefore, no migration problems exist under the cell operating conditions. The pore flooding and electrocatalyst problems do not exist. The SOFCs are said to have a good tolerance to overload, underload and short-circuiting.

Additional information on the features and tolerance to contaminants (e.g. sulfur) of a SOFC can be found in [1].

Our motivation behind the formulation presented in this paper is to guide the process design and development of an experimental laboratory-scale, high temperature fuel cell of the type sketched in ***Figure 1***. After the acquisition of such a system, it is here suggested to experimentally determine the fuel cell electrode electro-kinetics parameters first; such as the exchange current densities, i_0, at the cell electrode-electrolyte interfaces and the charge transfer coefficients, α_a and α_c, over the temperature range: 700-1100 K for the various fuel types mentioned above. The values of such electrode-kinetics related parameters are always required for the determination of the cell voltage loss due to the occurrence of the electrode electrochemical reactions for solid oxide fuel cell being operated at a constant current level.

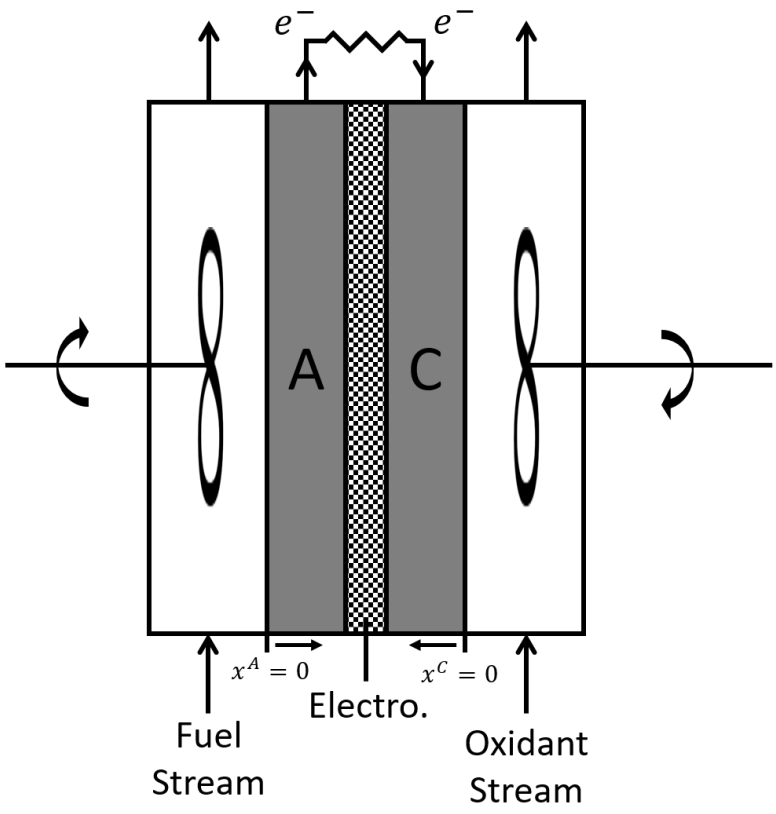

Figure 1. Sketch of a model high temperature solid oxide electrolyte fuel cell (not to scale)

The SOFC cell shown in ***Figure 1*** is explained as follows: The cell anode, A: It is a cermet of metallic nickel and yttria (Y_2O_3 (s)) stabilized zirconia (ZrO_2 (s)) with a porosity of 20-40% to facilitate the transport of reactant and product gaseous specious. The cell electrolyte, (denoted Electro.): Yttria-stabilized zirconia; yttria doping is required to stabilize the cubic crystal structure as well as for the creation of the oxygen vacancy defects required for the enhancement of ionic transport of the oxide ions in the solid state. A typical composition of the solid oxide electrolyte is: Yttria =16.9% (by weight) and zirconia = 83.1% (by weight). The cell cathode, C: Typical porous strontium-doped lanthanum manganite, $La_{1-x}Sr_xMnO_3$ $(0.10 < x < 0.18)$. The strontium doping bestows the *p*-type electronic conductivity by the creation *pf* electron holes. The electrode porosity facilitates the oxygen mass transport to the interface between the cell electrolyte and cathode. The fuel and oxidant species in the cell flow channels are stirred for their uniform distribution across the cross-sectional areas perpendicular to x-coordinate of the cell anode and cathode, respectively. Section 2 summarizes the theoretical formulation of the cell.

2. THEORETICAL FORMULATION

2.1. Formulation for the determination of the reactant and product species molar flow rates and their mole fractions

The formulation presented here assumes hydrogen gas as the cell fuel and air as the oxidant. It is also assumed that the current required from the cell is I amperes. Then, the cell anode and cathode geometric current densities are given by:

$$i_n^A = \frac{I}{A_{geom}^A} \quad and \quad i_n^C = \frac{I}{A_{geom}^C} \tag{1a, 1b}$$

Where A_{geom}^A and A_{geom}^C are the geometric areas between the cell electrolyte and anode, and cathode, respectively, perpendicular to the x-coordinate shown in ***Figure 1***.

At the cell anode electrode, the overall electrochemical reaction is:

$$H_2\,(g) + O^{2-} \rightarrow H_2O\,(v) + 2e^- \tag{2}$$

At the cell cathode electrode, the overall electrochemical reaction is:

$$\frac{1}{2}O_2\,(g) + 2e^- \rightarrow O^{2-} \tag{3}$$

For the galvanic SOFC delivering electric power to an external electrical load circuit, the net rates of the reactions, Eq. (2) and (3) are in the forward direction. The species consumption ($conv$) and production ($prod$) rates via these reactions are as follows:

$$\dot{n}_{H_2(g),conv}^A = \frac{i_n^A}{2F} = \frac{I}{2FA_{geom}^A} \quad ; \quad \left(moles\ of\ hydrogen\ gas\ consumed \cdot s^{-1} \cdot cm_{geom}^{-2}\right) \tag{4}$$

$$\dot{n}_{H_2O(v),prod}^A = \frac{i_n^A}{2F} = \frac{I}{2FA_{geom}^A} \quad ; \quad \left(moles\ of\ water\ vapor\ produced \cdot s^{-1} \cdot cm_{geom}^{-2}\right) \tag{5}$$

$$\dot{n}_{O^{2-},conv}^A = \frac{i_n^A}{2F} = \frac{I}{2FA_{geom}^A} \quad ; \quad \left(moles\ of\ oxide\ ions\ consumed \cdot s^{-1} \cdot cm_{geom}^{-2}\right) \tag{6}$$

$$\dot{n}_{O_2(g),conv}^C = \frac{i_n^C}{4F} = \frac{I}{4FA_{geom}^C} \quad ; \quad \left(moles\ of\ oxygen\ gas\ consumed \cdot s^{-1} \cdot cm_{geom}^{-2}\right) \tag{7}$$

$$\dot{n}_{O^{2-},prod}^C = \frac{i_n^C}{2F} = \frac{I}{2FA_{geom}^C} \quad ; \quad \left(moles\ of oxide\ ions\ produced \cdot s^{-1} \cdot cm_{geom}^{-2}\right) \tag{8}$$

The overall cell reaction is:

$$H_2\,(g) + \frac{1}{2}O_2(g) \rightarrow H_2O\,(v) \tag{9}$$

To deliver total cell current, I amperes, the required total hydrogen conversion rate is:

$$\dot{n}_{H_2(g),conv}^t = \frac{I}{2F} \quad ; \quad \left(total\ moles\ of\ hydrogen\ gas\ consumed \cdot s^{-1}\right) \tag{10}$$

The required total oxygen conversion rate is:

$$\dot{n}_{O_2(g),conv}^t = \frac{I}{4F} \quad ; \quad \left(total\ moles\ of\ oxygen\ gas\ consumed \cdot s^{-1}\right) \tag{11}$$

Assuming the hydrogen gas feed contains water vapor at the water vapor mole fraction $y_{H_2O(v),0}^A$; the hydrogen feed rate is:

$$\dot{n}^{t}_{H_2(g),0} = \left(1 - y^{A}_{H_2O(v),0}\right)\dot{n}^{t}_{moist\ H_2(g),0} \quad ; \quad \begin{pmatrix} total\ moles\ of\ hydrogen\ gas \\ fed \cdot s^{-1}\ to\ the\ anode \end{pmatrix} \tag{12}$$

Where,

$$\dot{n}^{t}_{moist\ H_2(g),0} = \begin{pmatrix} total\ molar\ feed\ rate\ of\ the\ mixture\ of\ hydrogen \\ and\ water\ vapor\ to\ the\ anode, moles \cdot s^{-1} \end{pmatrix}$$

The fractional conversion of hydrogen to produce the required amount of total cell current, I amperes is:

$$X_{H_2(g)} = \frac{\dot{n}^{t}_{H_2(g),conv}}{\dot{n}^{t}_{H_2(g),0}} \tag{13}$$

$$X_{H_2(g)} = \frac{\frac{I}{2F}}{\left(1 - y^{A}_{H_2O(v),0}\right)\dot{n}^{t}_{moist\ H_2(g),0}} \tag{14}$$

The total hydrogen molar flow rate at the cell anode-side flow channel exit is:

$$\dot{n}^{t}_{H_2(g),leav} = \dot{n}^{t}_{H_2(g),0} - \dot{n}^{t}_{H_2(g),conv} = \left(1 - y^{A}_{H_2O(v),0}\right)\dot{n}^{t}_{moist\ H_2(g),0} - \frac{I}{2F} \quad ; \quad (moles \cdot s^{-1}) \tag{15}$$

The total water vapor molar flow rate at the cell anode-side channel exit is:

$$\dot{n}^{t}_{H_2O(v),leav} = \dot{n}^{t}_{H_2O(v),0} + \begin{pmatrix} the\ water\ vapor\ entering\ the\ anode - side\ flow\ channel \\ from\ the\ porous\ cell\ anode\ where\ it\ is\ produced\ via \\ the\ occurence\ of\ the\ net\ electrochemical\ electron \\ producing\ (oxidation)\ reaction \end{pmatrix} \tag{16}$$

$$\dot{n}^{t}_{H_2O(v),leav} = y^{A}_{H_2O(v)}\dot{n}^{t}_{moist\ H_2(g),0} + \frac{I}{2F} \quad ; \quad (moles \cdot s^{-1}) \tag{17}$$

The rate of the gas mixture leaving the cell anode-side fuel channel is:

$$\dot{n}^{t}_{gas\ mix,leav} = \left(\left(1 - y^{A}_{H_2O(v),0}\right)\dot{n}^{t}_{moist\ H_2(g),0} - \frac{I}{2F}\right) + \left(y^{A}_{H_2O(v)}\dot{n}^{t}_{moist\ H_2(g),0} + \frac{I}{2F}\right) \tag{18}$$

Thus,

$$\dot{n}^{t}_{gas\ mix,leav} = \dot{n}^{t}_{moist\ H_2(g),0} \tag{19}$$

The mole fractions of the chemical species in the gas mixture leaving the fuel cell anode-side flow channel, are given as follows:

$$y^{A}_{H_2(g),leav} = y^{A}_{H_2(g),0}\left(1 - X_{H_2(g)}\right) \tag{20}$$

$$y^{A}_{H_2O(v),leav} = y^{A}_{H_2O(v),0} + y^{A}_{H_2(g),0} \cdot X_{H_2(g)} \tag{21}$$

To obtain the cell current at the level of I amperes, the required oxygen conversion rate is given by:

$$\dot{n}^{t}_{O_2(g),conv} = \frac{I}{4F} \quad ; \quad (moles \cdot s^{-1}) \tag{22}$$

Using the rule-of-thumb of '5 mole% of excess oxygen' in the air feed to the SOFC so that there is no deficiency of oxygen to consume the entire amount, if required, of hydrogen gas fed to the cell, the required oxygen feed rate to the cell cathode is:

$$\dot{n}^{t,C}_{O_2(g),0} = 1.05\left(\frac{I}{4F}\right) \quad ; \quad (moles \cdot s^{-1}) \tag{23}$$

Dry air molar feed rate to the cell on the cathode-side,

$$\dot{n}_{air,0}^{t,C} = \left(\frac{1}{0.21}\right)\dot{n}_{O_2(g),0}^{t,C} = 1.25\left(\frac{I}{F}\right) \quad ; \quad (moles \cdot s^{-1}) \tag{24}$$

Total oxygen molar feed rate to the cell on its cathode-side,

$$\dot{n}_{O_2(g),0}^{t,C} = 0.21\dot{n}_{air,0}^{t,C} = 0.2625\left(\frac{I}{F}\right) \quad ; \quad (moles \cdot s^{-1}) \tag{25}$$

Total nitrogen molar flow rate in the air feed to the cell on its cathode side,

$$\dot{n}_{N_2(g),0}^{t,C} = 0.79\dot{n}_{air,0}^{t,C} = 0.9875\left(\frac{I}{F}\right) \quad ; \quad (moles \cdot s^{-1}) \tag{26}$$

Total nitrogen molar flow rate in the gas mixture at the exit of the cell cathode-side flow channel,

$$\dot{n}_{N_2(g),leav}^{t,C} = \dot{n}_{N_2(g),0}^{t,C} = 0.9875\left(\frac{I}{F}\right) \quad ; \quad (moles \cdot s^{-1}) \tag{27}$$

Total oxygen molar flow rate in the gas mixture at the exit of the cell cathode-side flow channel,

$$\dot{n}_{O_2(g),leav}^{t,C} = \dot{n}_{O_2(g),0}^{t,C} - \dot{n}_{O_2(g),conv}^{t,C} = 0.2625\left(\frac{I}{F}\right) - \left(\frac{I}{4F}\right) =$$
$$= 0.0125\left(\frac{I}{F}\right) \quad ; \quad (moles \cdot s^{-1}) \tag{28}$$

Total gas mixture molar flow rate at the exit of the cell cathode-side flow channel,

$$\dot{n}_{gas\ mix,leav}^{t,C} = \dot{n}_{N_2(g),leav}^{t,C} + \dot{n}_{O_2(g),leav}^{t,C} =$$
$$= 0.9875\left(\frac{I}{F}\right) + 0.0125\left(\frac{I}{F}\right) \quad ; \quad (moles \cdot s^{-1}) \tag{29}$$

Thus,

$$\dot{n}_{gas\ mix,leav}^{t,C} = \frac{I}{F} \quad ; \quad (moles \cdot s^{-1}) \tag{30}$$

Oxygen mole fraction in the gas mixture at the exit of the cell cathode-side flow channel,

$$y_{O_2(g),leav}^{C} = \frac{\dot{n}_{O_2(g),leav}^{t,C}}{\dot{n}_{gas\ mix,leav}^{t,C}} = 0.0125 \tag{31}$$

Nitrogen mole fraction in the gas mixture at the exit of the cell cathode-side flow channel,

$$y_{N_2(g),leav}^{C} = \frac{\dot{n}_{N_2(g),leav}^{t,C}}{\dot{n}_{gas\ mix,leav}^{t,C}} = 0.9875 \tag{32}$$

2.2. Formulation for the determination of the SOFC Nernst voltage

The cell Nernst voltage, at a temperature T, is given by the following equation [3]:

$$E_T = E_T^{\circ} - \frac{RT}{nF}\ln\left(\prod_i (\hat{a}_i)^{\nu_i}\right) \quad ; \quad (volt) \tag{33}$$

Where,

$$\sum_i \nu_i A_i = 0 \tag{34}$$

Here $\hat{a}_i$ is the activity of a species involved in a cell or an electrode reaction, ν_i is the stoichiometric coefficient of species A_i involved in the cell or an electrode reaction (negative if consumed and positive if produced), F is Faraday's constant ($96487\ coulomb \cdot mol^{-1}$), n is the number of moles of electrons involved in the occurrence of one mole of an electrochemical reaction, R is the universal gas constant, E_T° is the standard-state electric potential associated with an electrochemical reaction occurring at a temperature T (K) when the activity of each species involved in the reaction is unity ($\hat{a}_i = 1$).
E_T° can be determined from the following equation,

$$E_T^\circ = \left(\frac{-\Delta G_T^\circ}{nF}\right) \quad ; \quad (volt) \tag{34a}$$

Where ΔG_T° is given by [4],

$$\frac{\Delta G_T^\circ}{RT} = \frac{\Delta G_0^\circ - \Delta H_0^\circ}{RT_0} + \frac{\Delta H_0^\circ}{RT} + \frac{1}{T}\int_{T_0}^{T}\left(\frac{\Delta C_p^\circ}{R}\right)dT - \int_{T_0}^{T}\left(\frac{\Delta C_p^\circ}{R}\right)dT \tag{35}$$

Where $\Delta G_T^\circ = \sum_i\left(\nu_i G_{i,T}^\circ\right)$ is the Gibbs free energy change of the reaction (Eq. (9)) at temperature T. ΔG_0° and ΔH_0° are standard quantities of the reaction at the reference temperature $T_0 = 298.15K$ and are defined in Eqs. (36a) and (36b):

$$\Delta G_0^\circ = \sum_i\left(\nu_i G_{i,T_0}^\circ\right) = \sum_i\left(\nu_i \Delta G_{f,i,T_0}^\circ\right) \tag{36a}$$

$$\Delta H_0^\circ = \sum_i\left(\nu_i H_{i,T_0}^\circ\right) = \sum_i\left(\nu_i \Delta H_{f,i,T_0}^\circ\right) \tag{36b}$$

$C_{p,i}^\circ$ is the standard-state heat capacity of species i at temperature T and its change due to reaction, ΔC_p° is defined in Eq. (36c):

$$\Delta C_p^\circ = \sum_i\left(\nu_i C_{p,i}^\circ\right) \tag{36c}$$

The enthalpy change of the reaction at temperature T is given by,

$$\Delta H_T^\circ = \Delta H_0^\circ + R\int_{T_0}^{T}\left(\frac{\Delta C_p^\circ}{R}\right)dT \tag{37}$$

Eq. (33) for the cell reaction represented by Eq. (9) leads to:

$$E_T = E_T^\circ - \left(\frac{RT}{nF}\right)\ln\left(\frac{\hat{a}_{H_2O(v)}}{\hat{a}_{H_2(g)}\hat{a}_{O_2(g)}^{0.5}}\right) \quad ; \quad (volt) \tag{38}$$

Where $\hat{a}_{H_2O(v)}$ and $\hat{a}_{H_2(g)}$ are the activity of water vapor and hydrogen gas, respectively, in the cell anode-side gas mixture in the fuel chamber at temperature T and total pressure P_t^A; and $\hat{a}_{O_2(g)}$ is the activity of oxygen gas in the gas mixture at temperature T and total pressure P_t^C in the cell cathode-side oxidant (air) chamber.

The activity of a species i in a gas mixture is given by,

$$\hat{a}_i = \frac{\hat{\phi}_i y_i P_t}{P^\circ} \tag{39}$$

Where, y_i is the mol fraction of species i in the gas mixture, P_t is the total pressure of the mixture, $P^\circ = 1\ bar$ (the standard-state pressure), and $\hat{\phi}_i$ is the fugacity coefficient of species i in the gas mixture which accounts for any non-ideal behavior. The formulation to calculate $\hat{\phi}_i$ is available in [4]. If the total pressure, P_t is less than 5 bar, it is appropriate to assume ideal behavior. Thus:

$$\hat{\phi}_i^A = \hat{\phi}_i^C = 1 \tag{40}$$

For this situation, Eq. (38) is expressed as:

$$E_T = E_T^\circ - \left(\frac{RT}{nF}\right)\ln\left(\frac{y^A_{H_2O(v)}}{y^A_{H_2(g)}\sqrt{y^C_{O_2(g)}}}\right) + \frac{RT}{2nF}\ln\left(\frac{P_t^C}{P^\circ}\right) \quad ; \quad (volt) \tag{41}$$

Eq. (41) is the Nernst equation for the cell with the fuel and oxidant mixtures in the ideal state.

2.3. Formulation for the determination of the cell electrode overpotentials, η_s, or the electrochemical kinetics polarization voltage losses associated with the occurrence of electrochemical reactions in the cell electrodes

The surface overpotential, η_s, for an electrochemical reaction associated with the charge transfer across the interface between the cell electrolyte and the active material of an electrode, is given by the celebrated Butler-Volmer equation:

$$i_{n,s} = i_0\left[\exp\left(\frac{\alpha_A F\eta_s}{RT}\right) - \exp\left(\frac{\alpha_C F(-\eta_s)}{RT}\right)\right] \quad ; \quad (amperes \cdot cm_s^{-2}) \tag{42}$$

Where $i_{n,s}$ is the interfacial current density normal to the interface between the electrolyte and the active material of a cell electrode, i_0 is the exchange current density for an electrochemical reaction occurring in a cell electrode ($amps \cdot cm^{-2}$). This depends on the composition of the reactive gas mixture adjacent to the cell electrode, as well as the temperature and nature of the electrode surface. Furthermore, $\alpha_A = (1-\beta)n$ and $\alpha_C = \beta n$ are the apparent charge transfer coefficient, respectively, for the charge transfer across the electrolyte-electrode interface in the anodic (oxidation or electron producing) and the cathodic (reduction or electron consuming) direction of an electrochemical reaction occurring at a finite rate.

By definition, the electrode surface overpotential is,

$$\eta_s = V - U \tag{43}$$

Where U is the reversible or Nernst electric potential at an electrode of a galvanic cell when $i_{n,s} = 0$ and V is the cell actual or operational electrode electric potential when the interfacial current density has a finite value except zero. The symmetry factor β represents a fraction of the actual electrode potential, V, which promotes the cathodic direction reaction. Similarly, $(1-\beta)$ is the fraction of the electric potential, V, which promotes the anodic direction reaction. In the absence of the exact values of α_A and α_C of an electrode electrochemical reaction, it is frequently assumed that $\beta = 0.5$ so that Eq. (42) reduces to:

$$i_{n,s} = i_0\left[\exp\left(\frac{nF\eta_s}{2RT}\right) - \exp\left(\frac{nF(-\eta_s)}{2RT}\right)\right] \quad ; \quad (amperes \cdot cm_s^{-2}) \tag{44}$$

Or,

$$\frac{i_{n,s}}{i_0} = \left[\exp\left(\frac{nF\eta_s}{2RT}\right) - \exp\left(-\frac{nF\eta_s}{2RT}\right)\right] \quad ; \quad (amperes \cdot cm_s^{-2}) \tag{45}$$

Which can be represented as,

$$\frac{i_{n,s}}{i_0} = 2\sinh\left(\frac{nF\eta_s}{2RT}\right) \tag{46}$$

For the electrode reactions in Eq. (2) and (3), $n = 2$, therefore Eq. 46 reduces to:

$$\frac{i_{n,s}}{i_0} = 2\sinh\left(\frac{F\eta_s}{RT}\right) \tag{47}$$

This is valid for each of the two electrodes in the galvanic cell.

During the period of the SOEFC delivering electric power to an external electrical load circuit; the net current density, $i_{n,s}^{A}$, at the cell-anode electrode is assumed to be positive along with the overpotential η_s^A being positive; whereas, the net current density, $i_{n,s}^{C}$, at the cell-cathode electrode is taken to be negative along with η_s^C being negative or $(-\eta_s^C)$ as positive.

By the use of Taylor series, Eq. (42) is expressed as:

$$\frac{i_{n,s}}{i_0} = \left[\frac{(\alpha_A + \alpha_C)F\eta_s}{RT} + \frac{1}{2!}(\alpha_A^2 - \alpha_C^2)\left(\frac{F\eta_s}{RT}\right)^2 + \cdots\right] \tag{48}$$

At small values of η_s, this reduces to:

$$\frac{i_{n,s}}{i_0} = \frac{(\alpha_A + \alpha_C)F\eta_s}{RT} \tag{49}$$

It is here noted that for a given reactive mixture composition adjacent to the cell electrode surface, there are three electrochemical reaction kinetic parameters: i_0, α_A, and α_C. For large values of η_s (e.g. $|\eta_s| > 0.1\ volt$), one of the terms in Eq. (42) is negligible relative to the other. The overall electrochemical reaction rate is then given by:

$$i_{n,s} = i_0 \exp\left(\frac{\alpha_a F\eta_s}{RT}\right), \quad \left(for\ (\alpha_a F\eta_s) \gg (RT)\right) \tag{50}$$

Or

$$i_{n,s} = -i_0 \exp\left(-\frac{\alpha_C F\eta_s}{RT}\right), \quad \left(for\ (\alpha_c F\eta_s) \ll (-RT)\right) \tag{51}$$

Eqs. (50) and (51) are known as the Tafel equations. On further rearrangement, Eq. (50) and (51) are now given as

$$\ln\left(\left|\frac{i_{n,s}}{i_0}\right|\right) = \left(\frac{\alpha_a F}{RT}\right)\eta_s \tag{52}$$

$$\ln\left(\left|\frac{-i_{n,s}}{i_0}\right|\right) = \left(\frac{\alpha_c F}{RT}\right)(-\eta_s) \tag{53}$$

The left-hand side of Eq. (52) plotted vs. η_s as well as that of Eq. (53) plotted vs. $(-\eta_s)$ would result in a straight line; the slope of which is $(\alpha_a F/RT)$ for Eq. (52) and $(\alpha_c F/RT)$ for Eq. (53). Using of experimental data, such plots can be developed and the slopes can be obtained thereby allowing for the determination of α_a and α_c. One is referred to reference [5] for more comprehensive information on the electrode reaction kinetics.

For the case of the porous electrodes of a galvanic fuel cell, the relation between $i_{n,s}$ and the geometric current density, $i_{n,geom}$, for each of its electrodes is

$$i_{n,s} = \frac{i_{n,geom}}{a_{eff}}, \quad (amp \cdot cm_s^2) \tag{54}$$

Where

$$a_{eff} = \begin{pmatrix} effective\ interfacial\ area\ between\ the\ cell \\ electrolyte\ and\ the\ grains\ of\ active\ material\ of\ an \\ electrode\ of\ the\ galvanic\ SOEFC, (cm_s^2 \cdot cm_{geom}^{-2}) \end{pmatrix} \tag{54a}$$

The effective interfacial area of each electrode of the cell is related to its thickness as follows:

$$a_{eff}^A = \ell^A a^A, \quad \left(cm_s^2 \cdot cm_{geom}^{-2}\right) \tag{55}$$

$$a_{eff}^{C} = \ell^{C} a^{C}, \quad \left(cm_s^2 \cdot cm_{geom}^{-2}\right) \tag{56}$$

Where ℓ^A and ℓ^C are the thicknesses of the anode and cathode electrode of the cell (cm), a^A and a^C are the effective interfacial area per unit volume of the anode and cathode electrode of the cell ($cm_s^2 \cdot cm_{electrode}^{-3}$). Furthermore, if the information on the effective interfacial area between the electrolyte and each cell electrode active material per gram of the composite electrode, S_g $(cm_s^2 \cdot g^{-1})$, is available; then:

$$a_{eff} = m_{geom}^{A} S_g^{A} \quad ; \quad a_{eff}^{C} = M_{geom}^{C} S_g^{C} \quad \left(cm_s^2 \cdot cm_{geom}^{-2}\right) \tag{57a, 57b}$$

Where m_{geom}^{A} and m_{geom}^{C} denote the mass of the cell composite anode and cathode electrodes per unit geometric area perpendicular to the *x*-coordinate shown in ***Figure 1***.

$$m_{geom}^{A} = \frac{m_{tot}^{A}}{A_{geom}^{A}} \quad ; \quad m_{geom}^{C} = \frac{m_{tot}^{C}}{A_{geom}^{C}} \quad \left(gm \cdot cm_{geom}^{-2}\right) \tag{58a, 58b}$$

2.4. Formulation for the determination of the ohmic voltage drops due to the transport of ions and electrons in the components of the model SOEFC sketched in Figure 1

The ohmic voltage drops in the anode, cathode, and electrolyte of the model cell are given, respectively, as follows:

$$\eta_{\Omega}^{A} = \ell^{A} \rho_{resist}^{A} i_{n,geom}^{A} \quad (volt) \tag{59a}$$

$$\eta_{\Omega}^{C} = \ell^{C} \rho_{resist}^{C} i_{n,geom}^{C} \quad (volt) \tag{59b}$$

$$\eta_{\Omega}^{E} = \ell^{E} \rho_{resist}^{E} i_{n,geom}^{E} \quad (volt) \tag{59c}$$

Where, ℓ^A, ℓ^C, ℓ^E represent the thickness of the cell anode, cathode, and electrolyte respectively (cm); ρ^A, ρ^C, ρ^E are the electrical resistivity of the cell anode, cathode, and electrolyte respectively $(\Omega \cdot cm)$; and $i_{n,geom}^{A}$, $i_{n,geom}^{C}$, $i_{n,geom}^{E}$ denote the geometric current density associate with the charge transport through the thickness of the cell anode, cathode, and electrolyte respectively $(amp \cdot cm_{geom}^{-2})$.

The total cell voltage loss associated with the occurrence of electrochemical reactions and transport of the charged species (electrons and ions) is given by:

$$E_{loss}^{tot} = [(\eta_s^A + \eta_s^C) + (\eta_{\Omega}^{A} + \eta_{\Omega}^{C} + \eta_{\Omega}^{E})] \quad (volt) \tag{60}$$

(Note: the cell electrodes are assumed to be thin in this presentation.) The predicted cell voltage for the SOFC delivering electric power to an external electric load is given by:

$$V^{cell} = E_T^{cell} - E_{less}^{tot} \quad (volt) \tag{61}$$

Where the Nernst cell voltage, E_T^{cell}, is given by Eq. (41).

The cell electric power delivery to an external electrical load circuit at a geometric current level of i_{geom} is given by:

$$\dot{P} = i_{geom} V^{cell} \quad \left(watts \cdot cm_{geom}^{-2}\right) \tag{62}$$

Maximum fuel cell efficiency when the cell is operated at temperature T (K) is:

$$E_{max}^{efficiency} = \frac{-\Delta G_T^{\circ}}{-\Delta H_T^{\circ}} \tag{63}$$

And the actual cell operational voltage efficiency is given by:

$$E_{voltage}^{efficiency} = \frac{V^{cell}}{E_T^{cell}} \tag{64}$$

While the actual cell thermal efficiency is:

$$E_{thermal}^{efficiency} = \frac{2FV^{cell}}{-\Delta H_T} \tag{64a}$$

The actual rate of thermal energy production due to the total cell voltage loss at the current level of i_{geom} is given by:

$$\dot{q} = i_{geom}E_{loss}^{tot} \quad (watts \cdot cm_{geom}^{-2}) \tag{65}$$

If a gas turbine engine is working between a high (source) temperature, T_h (K), and a low (sink) temperature, T_c (K), the gas turbine Carnot cycle engine efficiency is given by:

$$E_{Carnot}^{efficiency} = 1 - \frac{T_c}{T_h} \tag{66}$$

It is here suggested that all the cell efficiencies given in equations (63) through (64-a) be compared with the turbine Carnot cycle engine efficiency.

3. Simplified theoretical formulation-based equations employed to compute the theoretical model data

Using the species heat capacity information [4], Eq. (35) and (37) were reduced; for the overall cell reaction: $H_2(g) + \frac{1}{2}O_2(g) \rightarrow H_2O(g)$; to:

$$(-\Delta G_T^{\circ}) = 237720.7547 - 32.3498T + 0.0032T^2 + \frac{62940}{T} - 13.2899\ln\left(\frac{T}{298.15}\right) \tag{67}$$

$$(-\Delta H_T^{\circ}) = 237719.53 + 13.2899T - 0.0032217T^2 + \frac{125960}{T} \tag{68}$$

Inserting $(-\Delta G_T^{\circ})$ from Eq. (67) into Eq. (34) leads to:

$$E_T^{\circ,cell} = \frac{1}{nF}[237720.7547 - 32.3498T + 0.0032T^2 + \frac{62940.0}{T} - 13.2899\ln\left(\frac{T}{298.15}\right)] \tag{69}$$

For the reaction represented by Eq. (9), $n = 2$ g-equivalents per g-mole of the reaction, Eq. (9).

Inserting $(-\Delta G_T^{\circ})$, $(-\Delta H_T^{\circ})$, and $E_T^{\circ,cell}$, respectively, from Eq. (67), (68), and (69), into Eq. (63), (64), and (64-a) leads to:

$$E_{max}^{efficiency} = \frac{237720.7547 - 32.3498T + 0.0032T^2 + \frac{62940.0}{T} - 13.2899\ln\left(\frac{T}{298.15}\right)}{237719.53 + 13.2899T - 0.0032217T^2 + \frac{125960}{T}} \tag{70}$$

$$E_{voltage}^{efficiency} = \frac{V^{cell} \cdot 2F}{237720.7547 - 32.3498T + 0.0032T^2 + \frac{62940.0}{T} - 13.2899\ln\left(\frac{T}{298.15}\right)} \tag{71}$$

$$E_{thermal}^{efficiency} = \frac{V^{cell} \cdot 2F}{237719.53 + 13.2899T - 0.0032217T^2 + \frac{125960}{T}} \tag{72}$$

By combining Eqs. (20), (21), and (31) we obtain:

$$\left(\frac{y_{H_2O(v)}^A}{y_{H_2(g)}^A \sqrt{y_{O_2(g)}^C}}\right) = 8.9443 \left(\frac{\frac{y_{H_2O(v)}^A}{y_{H_2(g)}^A} + X_{H_2(g)}}{1 - X_{H_2(g)}}\right) \tag{73}$$

Therefore:

$$\ln\left(\frac{y_{H_2O(v)}^A}{y_{H_2(g)}^A \sqrt{y_{O_2(g)}^C}}\right) = 2.1910 + \ln\left(\frac{\frac{y_{H_2O(v)}^A}{y_{H_2(g)}^A} + X_{H_2(g)}}{1 - X_{H_2(g)}}\right) \tag{74}$$

Inserting the information from Eq. (74) into Eq. (41) leads to:

$$E_T = E_T^\circ - \left(\frac{RT}{nF}\right)\left[2.1910 + \ln\left(\frac{\frac{y_{H_2O(v)}^A}{y_{H_2(g)}^A} + X_{H_2(g)}}{1 - X_{H_2(g)}}\right)\right] + \frac{RT}{2nF}\ln\left(\frac{P_t^C}{P^\circ}\right) \quad ; \quad (volt) \tag{75}$$

For dry hydrogen feed to the cell, $y_{H_2O(v)}^A = 0$ and Eq. (75) reduces to:

$$E_T = E_T^\circ - \left(\frac{RT}{nF}\right)\left[2.1910 + \ln\left(\frac{X_{H_2(g)}}{1 - X_{H_2(g)}}\right)\right] + \frac{RT}{2nF}\ln\left(\frac{P_t^C}{P^\circ}\right) \quad ; \quad (volt) \tag{76}$$

This is valid for the reaction in Eq. (9) with $n = 2$ and $X_{H_2(g)} \in [0,1]$.

Note that the hydrogen fractional conversion, $X_{H_2(g)}$, is related to the total cell current by the following equation,

$$X_{H_2(g)} = \frac{mols\ of\ hydrogen\ gas\ converted\ via\ reaction\ per\ second}{hydrogen\ molar\ feed\ rate\ to\ the\ cell\ anode - side\ channel\ per\ second} \tag{77}$$

Thus:

$$X_{H_2(g)} = \frac{\left(\frac{I}{2F}\right)}{\dot{n}_{H_2(g),0}^{t,A}} \tag{77a}$$

The rate of thermal energy production per unit geometric area due to the occurrence of the overall cell reaction, Eq. (9), if all of the hydrogen fuel is oxidized to produce only thermal energy, is given by:

$$\dot{q}_{only\ thermal} = (-\Delta H_T) \times (mol\ of\ reaction) \quad ; \quad \left(watt \cdot cm_{geom}^{-2}\right) \tag{78}$$

$$\dot{q}_{only\ thermal} = \left(237719.53 + 13.2899T - 0.0032217T^2 + \frac{125960}{T}\right)\left(\frac{i_{n,geom}}{2F}\right) \tag{78a}$$

The change in the standard-state entropy due to the occurrence of the overall cell reaction, Eq. (9),
is given by

$$\Delta S^{\circ}_{T_0} = S^{\circ}_{H_2O(g)} - \left(S^{\circ}_{H_2(g)} + \frac{1}{2}S^{\circ}_{O_2(g)}\right) \tag{79}$$

Using the species entropy data [7] at $T_0 = 298.15\ K$,

$$\Delta S^{\circ}_{T_0} = -44.385\ \frac{J}{mol \cdot K} \tag{80}$$

The standard-state entropy of a species [4] at temperature, T, is given by:

$$S^{\circ}_{i,T} = S^{\circ}_{T_0} + \int_{T_0}^{T} \frac{C^{ig}_{p,i}}{T}\, dT \tag{81}$$

$$S^{\circ}_{i,T} = S^{\circ}_{T_0} + R\left[A_i \ln\left(\frac{T}{T_0}\right) + B_i(T - T_0) + \frac{C_i}{2}(T^2 - T_0^2) - \frac{D_i}{2}\left(\frac{1}{T^2} - \frac{1}{T_0^2}\right)\right] \tag{81a}$$

Change in entropy associated with the occurrence of the reaction, Eq. (9), at temperature, $T[K]$,
Is given by:

$$\Delta S^{\circ}_{T} = \sum_i \nu_i\, S^{\circ}_{i,T} = S^{\circ}_{T_0} + R\left[\Delta A \ln\left(\frac{T}{T_0}\right) + \Delta B(T - T_0) + \frac{\Delta C}{2}(T^2 - T_0^2) - \frac{\Delta D}{2}\left(\frac{1}{T^2} - \frac{1}{T_0^2}\right)\right]$$

$$where$$

$$\Delta A = \sum_i \nu_i\, A_i = -1.5985$$

$$\Delta B = \sum_i \nu_i\, B_i = 0.000775 \tag{82}$$

$$\Delta C = \sum_i \nu_i\, C_i = 0.0$$

$$\Delta D = \sum_i \nu_i\, D_i = 15150$$

Combining the information provided in Eq. (80) and (82) leads to:

$$-\Delta S^{\circ}_{T} = 45.598 + 13.2899 \ln\left(\frac{T}{298.15}\right) - 0.00644T + \frac{62979}{T^2} \tag{83}$$

Where the cell temperature is in K.

The 'reversible' thermal energy production per g-mole occurrence of the overall cell reaction, Eq. (9), at temperature, $T[K]$,

$$q^{rev\ thermal}_{per\ mol} = T(-\Delta S^{\circ}_{T}) = 45.598T + 13.2899T \ln\left(\frac{T}{298.15}\right) - 0.00644T^2 + \frac{62979}{T} \tag{84}$$

The ratio of $q^{rev\ thermal}_{per\ mol}$ to $(-\Delta H^{\circ}_{T})$ is given as:

$$r = \frac{q^{rev\ thermal}_{per\ mol}}{(-\Delta H^{\circ}_{T})} = \frac{45.598T + 13.2899T \ln\left(\frac{T}{298.15}\right) - 0.00644T^2 + \frac{62979}{T}}{237719.53 + 13.2899T - 0.0032217T^2 + \frac{125960}{T}} \tag{85}$$

Where the cell temperature is in K.

4. Computed data for a typical formulation-based SOEFC and brief discussion

Figure 2 shows the Nernst cell electric voltage, E_T^{cell}, plotted versus the hydrogen fuel fractional conversion, $X_{H_2(g)}$, at three temperatures: 800, 1000, and 1100 K.

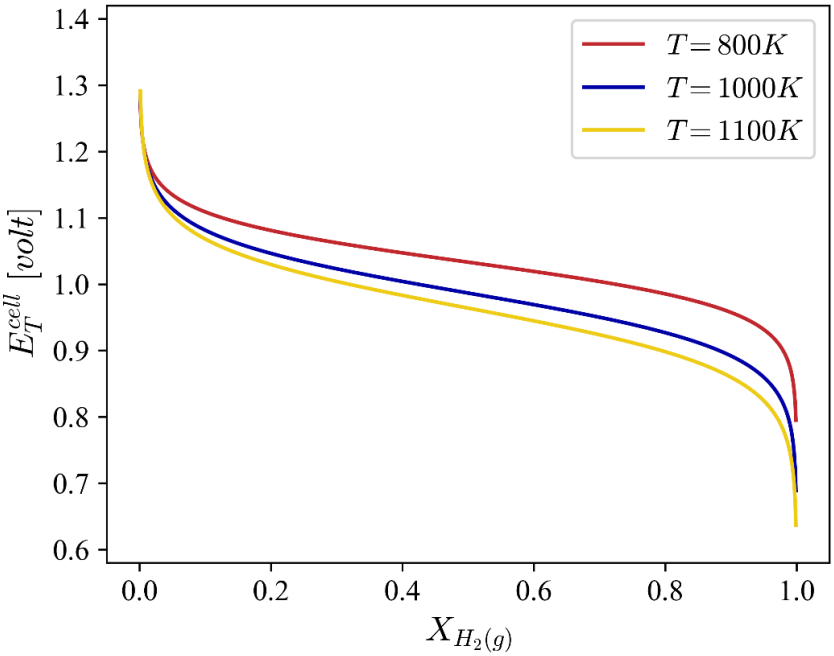

Figure 2. The open circuit cell voltage vs. hydrogen fuel fractional conversion at $\frac{P_t^C}{P^o} = 1$

At each value of the hydrogen fuel fractional conversion, the Nernst cell voltage decreases with an increase in the cell temperature. Also, at each cell temperature; the Nernst voltage decreases with an increase in the hydrogen fractional conversion in the manner shown in the plots. The plots in ***Figure 3*** at $\frac{P_t^C}{P^\circ} = 10$ are similar to those shown ***Figure 2*** at $\frac{P_t^C}{P^\circ} = 1$.

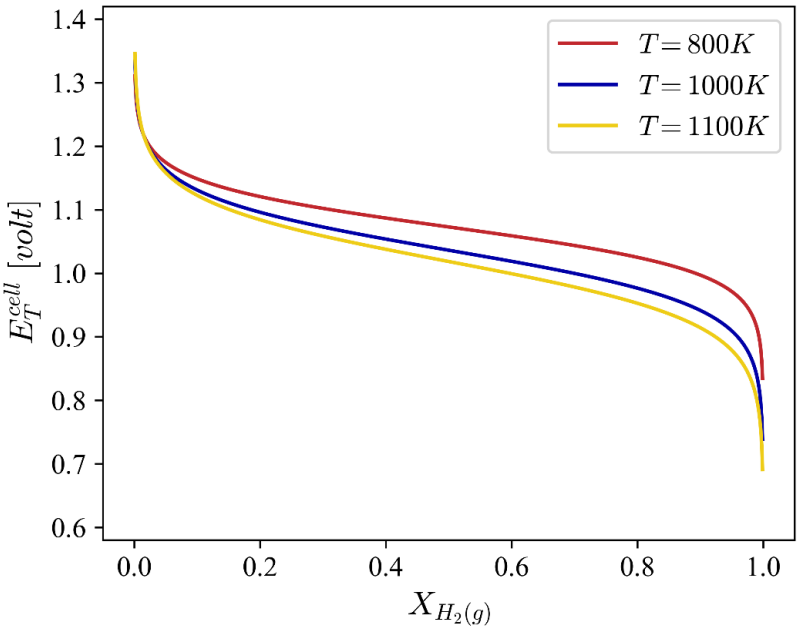

Figure 3. The open circuit cell voltage vs. hydrogen fuel fractional conversion at $\frac{p_t^C}{p^o} = 10$

The Nernst cell voltage in ***Figure 3*** is slightly higher than that in ***Figure 2*** for each set of the values of the cell temperature and the hydrogen fuel conversion. Thus, the effect of an increase in the oxidant reactant total pressure on the cell open circuit voltage is demonstrated.

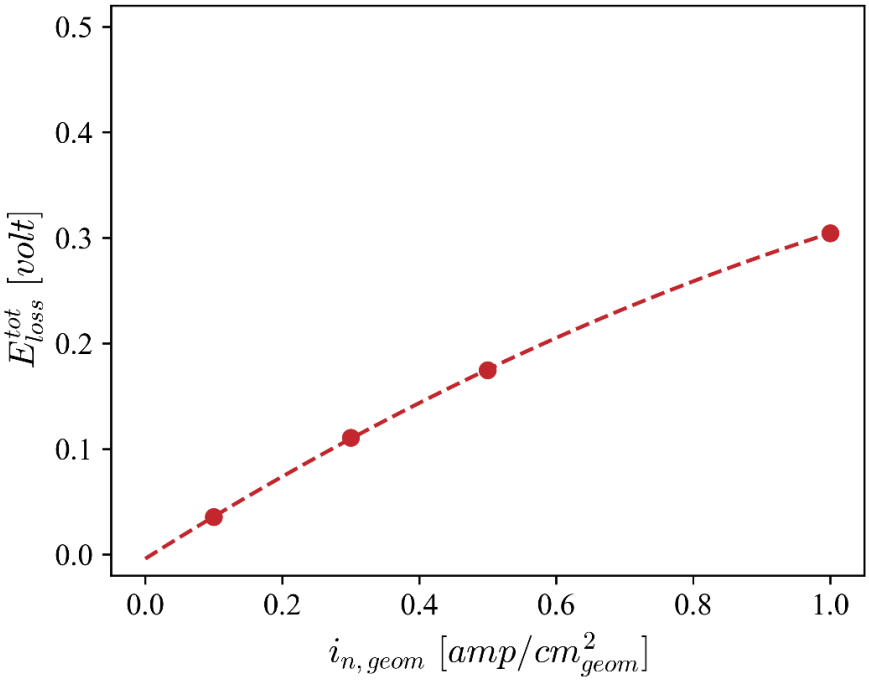

Figure 4. The SOFC operational voltage loss at $T = 1100K$

Figure 4 is the plot of the calculated total cell voltage loss [2, 6], E_{loss}^{tot}, versus the cell geometric current density, $i_{n,geom}$, at the cell operational temperature of 1100 K. At low geometric current densities, the relation of the cell total voltage loss with the geometric current density is a straight-line behavior; whereas at higher current densities, it is non-linear. This is the representation of the effect of the cell electrochemical reaction polarization voltage loss on the total cell voltage loss which accounts for all the cell voltage losses due to the transport of electronic and ionic species in the various cell components and the electrochemical reaction polarization voltage losses at the both cell electrodes.

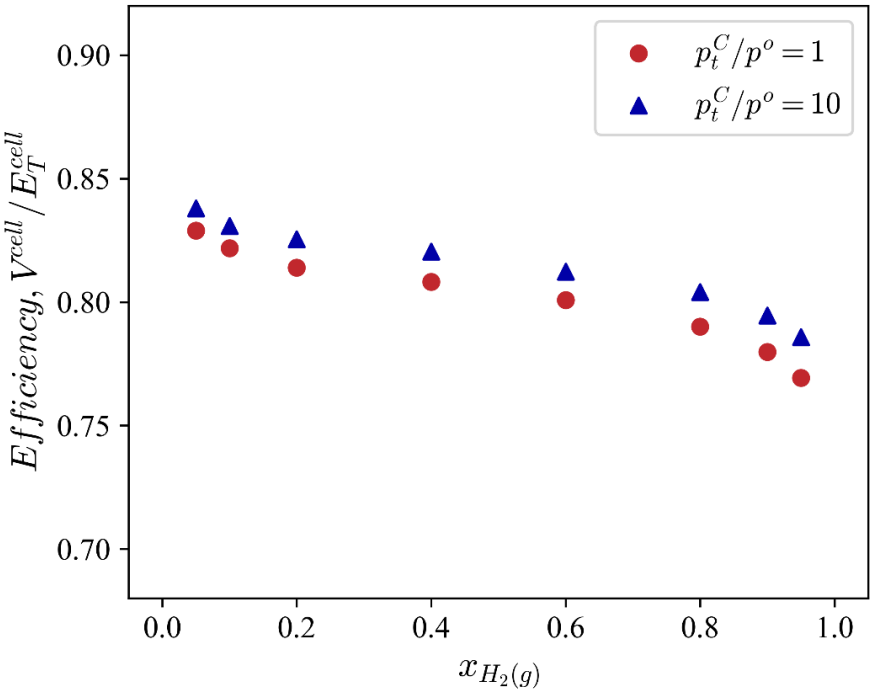

Figure 5. The SOFC operational voltage efficiency vs the hydrogen fuel fractional conversion

Figure 5 shows the plots of the cell electric voltage efficiency, $E_{volt}^{eff} = \frac{V^{cell}}{E_T^{cell}}$ versus the hydrogen fuel fractional conversion for the cell geometric current density of 0.5 $amp \cdot cm_{geom}^{-2}$ at the cell operational temperature of 1100 K at $\frac{P_t^C}{P^\circ} = 1$ and $\frac{P_t^C}{P^\circ} = 10$. The profile at higher cathode-side oxidant total pressure of 10 bar lies above that at lower cathode-side total pressure of 1 bar. The cell electric voltage efficiency is a fractional measure of the overall cell reaction's Gibbs free energy change, associated with the oxidation of a fuel (here, hydrogen fuel), to produce electrical energy.

Figure 6 is the plot of r versus the cell operational temperature. Here r is defined as below:

$$\left[r = \frac{\begin{pmatrix} reversible\ thermal\ energy\ or\ heat\ production\ associated\ with\ the \\ entropy\ change\ due\ to\ the\ occurence\ of\ the\ overall\ cell\ reaction \\ at\ the\ cell\ temperature\ T \end{pmatrix}}{\begin{pmatrix} total\ thermal\ energy\ production\ associated\ with\ the\ enthalpy \\ change\ due\ to\ the\ occurence\ of\ the\ same\ overall\ cell\ reaction \\ at\ the\ same\ cell\ temperature\ T \end{pmatrix}} \right]$$

The linear relation of r with the cell temperature is quite apparent. This quantity r is indicative of the ratio of the reaction reversible heat generated to the total thermal energy generated if the fuel is assumed to be completely converted to the final product species (here, water vapor from the hydrogen fuel used in the current analysis).

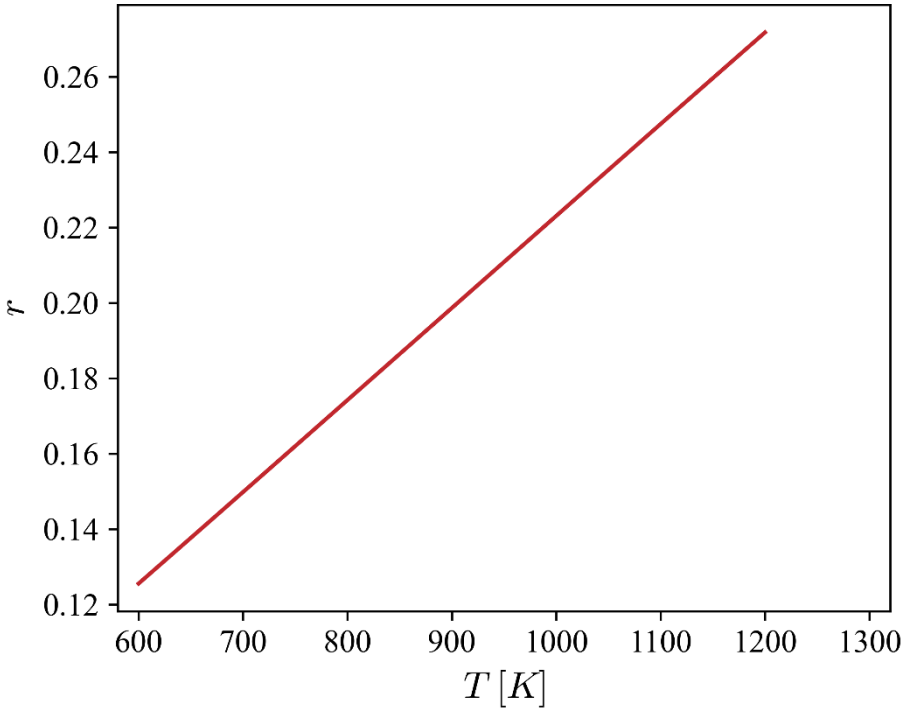

Figure 6. The ratio of the thermal energy production due to the change in entropy to that in enthalpy because of the occurrence of the SOFC overall reaction, Eq. (9).

Figure 7 shows the plots of the rate of thermal energy production, $\dot{q}_{thermal}$ versus the cell geometric current density, $i_{n,geom}$, at an operational temperatures of 800 K. The relation of the thermal energy production rate (assuming that the cell fuel (hydrogen) is oxidized completely to final product species, water vapor) with the geometric current density is linear. Similar data at operational temperatures of 1000 K and 1100 K overlap the data shown due to insignificant changes in the enthalpy of the overall cell reaction.

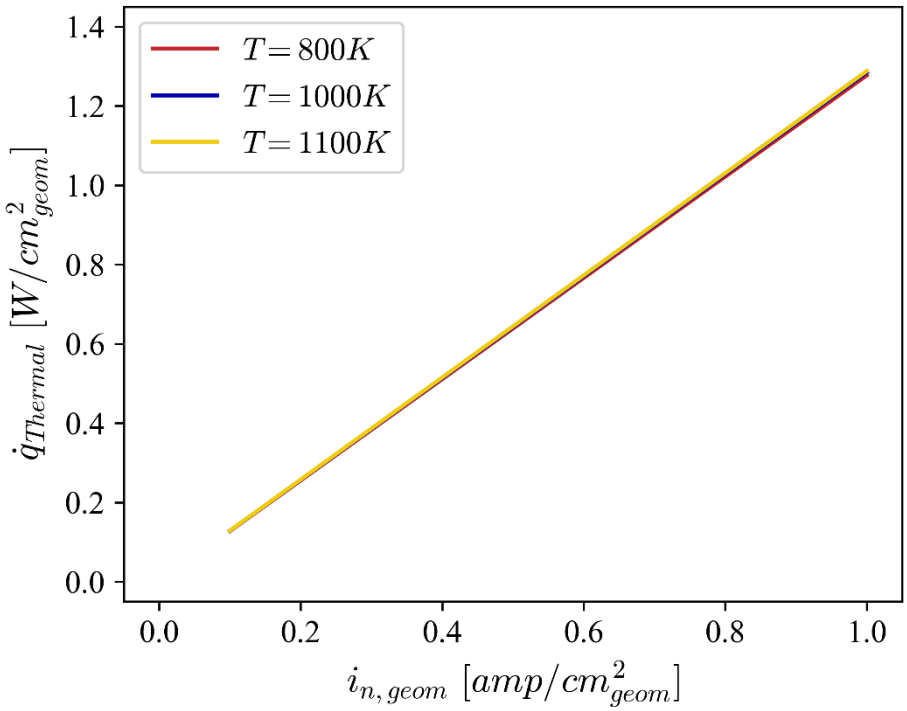

Figure 7. Rate of thermal energy production with the enthalpy change due to the overall reaction, Eq. (9) vs the geometric current density

Three relevant thermal efficiencies are defined as follows:

$$E^{eff}_{max} = \left(\frac{\Delta G^{\circ}_{T}}{\Delta H^{\circ}_{T}}\right) \quad ; \quad E^{eff}_{actual} = \left(\frac{2FV^{cell}}{-\Delta \mathrm{H}^{\circ}_{\mathrm{T}}}\right) \quad ; \quad E^{eff}_{Carnot} = \left(1 - \frac{T_c}{T_h}\right)$$

.

At a cell operational temperature of 1100 K, the maximum and Carnot cycle thermal efficiency are, 79.08% and 62.90%, respectively. The Carnot cycle engine thermal efficiency was calculated using the sink thermal reservoir temperature, $T_c = 408.15\ K$. The high temperature SOFC's actual thermal efficiency for its operation at the geometric current density, $i_{n,geom} = 0.5\ amp \cdot cm^{-2}_{geom}$, $\frac{P^C_t}{P^{\circ}} = 1$, and $T = 1100\ K$ is shown in **Table 1**.

Table 1. Calculated thermal efficiencies of the SOFC at various hydrogen fractional conversions

Hydrogen fractional conversion, $X_{H_2(g)}$	0.05	0.10	0.20	0.40	0.60	0.80	0.90
Predicted cell terminal voltage, V^{cell}	0.8323	0.7969	0.7585	0.7120	0.6735	0.6271	0.5886
E^{eff}_{actual}	0.6793	0.6504	0.6190	0.5811	0.5496	0.5118	0.4804

Three types of thermal efficiencies as shown above should be computed and compared. The comparison of the cell actual thermal efficiency to the Carnot cycle engine-based thermal efficiency would give the information about the gap between them; thus, providing very useful information with regard to arriving at the decision in the selection of an electric power system, a high temperature SOFC or a Carnot cycle-based heat engine. Based on the difference between the cell

maximum and actual thermal efficiencies, a fuel cell designer can modify the cell design to change the hydrogen fractional conversion for a fixed set of values of reactant total pressures, temperature, and geometric current density to achieve a desired cell performance.

5. CONCLUDING REMARKS

The assembled/ developed formulation for a high temperature SOEFC presented in Section 2 was used to compute the data with hydrogen gas as its fuel. Some typical predicted data were presented in the form of plots in Section 4. The following conclusions are drawn from the predicted data.

(a) The Nernst cell electric potential decreases with an increase in the cell's operational temperature range: 800 through 1100 K. Also, this electric potential decreases with an increase in the hydrogen fuel fractional conversion.

(b) For each set of temperature and hydrogen fractional conversion, the Nernst cell electric potential is higher at a higher cell cathode-side oxidant total pressure.

(c) The relation between the total cell voltage loss and geometric current density is linear at lower geometric current densities; it is nonlinear at higher geometric current densities.

(d) The electric voltage efficiency of the cell (a measure of the fractional utilization of the Gibbs free energy change associated with the occurrence of the overall reaction) is higher at a higher cathode-side oxidant pressure.

(e) The ratio of the reversible heat to the thermal energy production due to the occurrence of the overall cell reaction increases in a linear way with an increase in the cell operational temperature.

(f) The rate of the thermal energy production, associated with the overall cell reaction enthalpy change, increases linearly with an increase in the cell geometric current density at an operational cell temperature.

(g) The maximum thermal efficiency is greater than the SOFC actual thermal efficiency.

(h) The formulation, presented in this paper, can be conveniently adapted for the performance analysis of a high temperature SOEFC being fed with a fuel, such as: methane, natural gas, syn-fuel, hydrazine, octane, etc.

It is here suggested that after the validation of the fundamental theory-based formulation presented in this paper using the carefully acquired accurate experimental data, it be compared with the model previously appeared in the literature, for example, in the reference [8]. It is hoped that such a comparison would clearly illustrate the level of accuracy of each model to predict the performance of a high temperature solid oxide-electrolyte fuel cell to deliver electric power to an external electric load over the cell operational temperature range of 700-1100 K.

REFERENCES

1. A.J. Appleby and F.R. Foulkes, Fuel cell Handbook, pp.579-611, Van Nostrand Reinhold (1989).
2. J. Larminie A. Dicks, Fuel Cell Systems Explained, pp. 208-226, J. Wiley & Sons Ltd (2003).
3. G. Prentice, Electrochemical Engineering Principles, p. 37, Prentice-Hall, Inc. (1991)
4. J.M. Smith, et al. Introduction to Chemical Engineering Thermodynamics, pp. 535,366-382, 182, McGraw-Hill education. (2018, 8th edition).
5. J. Newman and N.P. Balsara, Electrochemical Systems, pp. 167-201, John Wiley & Sons, Inc. (2021, 4th edition).
6. B. Sunde'n and M. Faghri (editors), Transport Phenomena in Fuel Cells, p.14. WIT Press (2005); Southampton, UK and Billerica, MA, USA.
7. G.M. Barrow, Physical Chemistry, pp.779-782. McGraw-Hill Book Company (1973, 3rd edition).
8. A. Yahya, et al., Electrochemical performance of solid oxide fuel cell: Experimental study and calibrated model. Energy, Vol. 142, 1 January 2018, pp. 932-943. https://doi.org/10.1016/j.energy.2017.10.088